⌘ *Author's Choice*

THE JOURNAL OF BIOLOGICAL CHEMISTRY VOL. 285, NO. 30, pp. 22927–22935, July 23, 2010

Two Novel Src Homology 2 Domain Proteins Interact to Regulate *Dictyostelium* Gene Expression during Growth and Early Development*[S]

Received for publication, May 3, 2010 Published, JBC Papers in Press, May 10, 2010, DOI 10.1074/jbc.M110.139733

Christopher Sugden[‡], Susan Ross[‡], Gareth Bloomfield[§], Alasdair Ivens[¶], Jason Skelton[¶], Annette Mueller-Taubenberger[‖], and Jeffrey G. Williams[‡1]

From the [‡]School of Life Sciences, University of Dundee, Dow Street, Dundee DD1 5EH, Scotland, United Kingdom, the [§]Wellcome Trust Sanger Institute, Hinxton CB10 1SA, United Kingdom, the [¶]Medical Research Council Laboratory of Molecular Biology, Hills Road, Cambridge CB2 2QH, United Kingdom, and the [‖]Institute for Cell Biology and Center for Integrated Protein Science, Munich, Ludwig Maximilians University, Schillerstrasse 42, D-80336 Munich, Germany

There are 13 *Dictyostelium* Src homology 2 (SH2) domain proteins, almost 10-fold fewer than in mammals, and only three are functionally unassigned. One of these, LrrB, contains a novel combination of protein interaction domains: an SH2 domain and a leucine-rich repeat domain. Growth and early development appear normal in the mutant, but expression profiling reveals that three genes active at these stages are greatly underexpressed: the *ttdA* metallohydrolase, the *abcG10* small molecule transporter, and the *cinB* esterase. In contrast, the multigene family encoding the lectin discoidin 1 is overexpressed in the disruptant strain. LrrB binds to 14-3-3 protein, and the level of binding is highest during growth and decreases during early development. Comparative tandem affinity purification tagging shows that LrrB also interacts, via its SH2 domain and in a tyrosine phosphorylation-dependent manner, with two novel proteins: CldA and CldB. Both of these proteins contain a Clu domain, a >200-amino acid sequence present within highly conserved eukaryotic proteins required for correct mitochondrial dispersal. A functional interaction of LrrB with CldA is supported by the fact that a *cldA* disruptant mutant also underexpresses *ttdA*, *abcG10*, and *cinB*. Significantly, CldA is itself one of the three functionally unassigned SH2 domain proteins. Thus, just as in metazoa, but on a vastly reduced numerical scale, an interacting network of SH2 domain proteins regulates specific *Dictyostelium* gene expression.

Interactions of SH2[2] domains with their phosphotyrosine-containing binding sites are integral to many metazoan signal transduction pathways (1). As one measure of this, the human genome encodes 110 SH2 domain proteins (2). In contrast, *Dictyostelium* encodes only 13 SH2 domain proteins (3), and *Arabidopsis* encodes just two definitively assigned SH2 domain proteins, both of unknown function (4, 5). Because the ancestor of *Dictyostelium* diverged from the lineage leading to animals at some time after the divergence of ancestral plants (6), this implies a massive expansion in SH2 domain-based signaling during the evolution of the metazoa. In support of this notion, the choanoflagellate *Monosiga brevicollis*, a close relative of the metazoa, encodes ~80 SH2 domain proteins (7).

Dictyostelium is an amoebozoan, but it is facultatively multicellular. When food is plentiful, individual cells grow and divide, but when the food supply is exhausted, they aggregate together to form a fruiting body composed of a cellular stalk supporting a mass of spores. It is the only non-metazoan organism where SH2 domain-phosphotyrosine signaling pathways have been functionally investigated. Four of the *Dictyostelium* SH2 domain proteins are STATs (8), five are predicted dual specificity kinases (9), and one is an orthologue of the Cbl proto-oncogene (10). The remaining three, FbxB, CldA, and LrrB, are of unknown function and have domain architectures that are not represented in metazoan SH2 domain proteins. FbxB contains an F-box and ankyrin repeats; F-boxes are targeting signals for ubiquination, and ankyrin repeats are protein-protein interaction domains. CldA contains a tetracopeptide repeat (a protein-protein interaction domain), and LrrB contains leucine-rich repeats (also protein-protein interaction domains).

Functional analysis of the *Dictyostelium* SH2 domain proteins has revealed a general similarity to the metazoan signaling paradigms but with several unexpected twists. STATb, for example, contains a leucine residue at the position of the universally conserved SH2 domain arginine that is primarily responsible for phosphotyrosine binding (11). Also, the level of tyrosine phosphorylation of STATc increases by regulated deactivation of a tyrosine phosphatase rather than, as in the metazoan STATs, by the activation of a tyrosine kinase (12). Thus, a better understanding of the *Dictyostelium* proteins can provide insights into the origin, diversity, and wider potentialities of SH2 domain signaling.

Metazoan SH2 domains act as components of signaling networks, often interacting with other SH2 domain-containing proteins, but *Dictyostelium* equivalents of the SH2 domain-

* This work was supported by Biotechnology and Biological Sciences Research Council Project Grant BB/C500428/1 and by Wellcome Trust Program Grant 06724.

⌘ *Author's Choice*—Final version full access.

[S] The on-line version of this article (available at http://www.jbc.org) contains supplemental Figs. S1–S3.

[1] To whom correspondence should be addressed: School of Life Sciences, University of Dundee, Dow St., Dundee DD1 5EH, United Kingdom. Tel.: 44-1382-385823; Fax: 44-1382-344111; E-mail: j.g.williams@dundee.ac.uk.

[2] The abbreviations used are: SH2, Src homology 2; STAT, signal transducers and activators of transcription; BisTris, 2-[bis(2-hydroxyethyl)amino]-2-(hydroxymethyl)propane-1,3-diol; TLCK, N^{α}-*p*-tosyl-L-lysine chloromethyl ketone; RT, reverse transcription; QPCR, quantitative real-time PCR; TAP, tandem affinity purification; GFP, green fluorescent protein.

containing receptors, adaptors, and targeting proteins that typify such networks have yet to be identified. The functionally unassigned SH2 domain proteins are obvious candidates for these roles. We focus our efforts on LrrB and provide evidence for a signaling network, involving CldA and in a pathway that regulates specific gene expression.

EXPERIMENTAL PROCEDURES

Cell Culture, Transformation, Development, and Gene Disruption—Dictyostelium discoideum strain Ax2 was grown axenically and transformed as described (13, 14). For development, axenically growing cells (1–5 $\times$ 10^6 cells/ml) were washed twice in 20 mM K_2HPO_4/KH_2PO_4, pH 6.2 (KK2), and resuspended at 1 $\times$ 10^8 cells/ml. Cells were either spotted or spread onto 1.5% (w/v) water agar or spread onto nitrocellulose HA filters (Millipore) at an approximate density of 3 $\times$ 10^6 cells/ml and left to develop at 22 °C. Transformant pools were selected at 20 μg/ml Geneticin, 30 μg/ml hygromycin, or 10 μg/ml blasticidin as appropriate.

Plasmid Construction—The *lrrB* gene (DDB_G0287823 in dictyBase, available on the World Wide Web) was disrupted using the full-length genomic sequence with a hygromycin resistance cassette replacing 900 bp of sequence, between 431 and 1330, including the coding sequence for the SH2 domain. A *cldA* (DDB_G0278895) disruption construct was constructed by random insertion (position 2109 bp) of a transposon (15) containing a blasticidin cassette into a 2.1-kb cloned genomic fragment of *cldA* (298–2442 bp). It was used to generate a disruptant of the *cldA* gene in Ax2. LrrB-GFP was constructed by inserting a full-length *lrrB* fragment (4–3180 bp) into Act15p-GFP,[3] producing an N-terminally GFP-tagged LrrB fusion protein. All of the C-terminal tandem affinity purification (TAP) tagging constructs used were derived from a *Dictyostelium* CTAP construct (16). LrrB-CTAP was constructed by inserting a 3.2-kb full-length genomic fragment (minus start and stop codons) of *lrrB* into the BamHI and XbaI cloning sites in CTAP. ΔCLrrB-CTAP was constructed by inserting a C-terminally truncated, 2.8-kb genomic fragment (4–2856 bp) of *lrrB* into the BamHI and XbaI cloning sites of CTAP. For LrrB-CTAP-mutR, a point mutation (coding for an alanine rather than an arginine at residue 198) was introduced into a full-length genomic *lrrB* fragment, lacking start and stop codons, by PCR. CldA-CTAP was constructed by inserting a 3.8-kb genomic fragment (298–4073 bp) of *cldA* into the BamHI and XbaI cloning sites of CTAP.

Reverse Transcription (RT)-PCR—Total cell RNA was prepared using the RNeasy minikit (Qiagen) with on-column DNA digestion from, typically, 1 $\times$ 10^7 cells. RT-PCR was performed using the Titanium One-Step RT-PCR kit (BD Biosciences).

Western Transfer Analysis and Quantification—For Western analysis, samples were separated by SDS-PAGE on a 4–12% BisTris precast gel (Invitrogen), blotted onto Hybond-C extra (GE Healthcare), and probed with one of the following primary antibodies: anti-14-3-3 rabbit polyclonal antibody or the commercial anti-phosphotyrosine antibodies P-Tyr-100 (Cell Signaling Technologies), 4G10 (Upstate) mouse anti-GFP (Roche Applied Science), or rabbit anti-TAP (Thermo Scientific). Horseradish peroxidase-coupled goat anti-mouse and anti-rabbit, IgG secondary antibodies (Bio-Rad) were used accordingly, with ECL detection (SuperSignal (Thermo Scientific)). IRDye™ 800-conjugated goat anti-rabbit IgG (H&L) (Rockland Immunochemicals) secondary antibody was also used with the anti-14-3-3 primary antibody and quantified using an Odyssey infrared imaging system (LI-COR Biosciences).

Microarray Design, Data, and Quantitative Real-time PCR (QPCR) Analysis—The microarray bears 9247 PCR products derived from *D. discoideum* open reading frames, all printed in duplicate (17). They non-redundantly cover 8579 predicted genes of the total of ~10,300 estimated genes (18). Three separate biological replicate experiments were performed, and the data were analyzed using Gene Spring software (Agilent Technologies). The design of the microarray used in this study is available from the ArrayExpress data base, accession E-TABM-803; the raw and normalized data have been stored in the same data base. Real-time QPCR was performed to analyze relative gene expression levels. RNA was prepared using the RNeasy minikit (Qiagen) with on-column DNA digestion from, typically, 1 $\times$ 10^7 cells. RNA was transcribed into cDNA using the ImProm II reverse transcriptase system (Promega), and QPCR was performed using iQ SYBR Green Supermix (Bio-Rad) on a Realplex^2 Thermo-cycler (Eppendorf). Vegetative Ax2 RNA was typically used as a reference, and all gene expression levels were normalized to the Ig7 expression level in the same sample. The primers used are presented in the figure legends.

Generation of Polyclonal Anti-14-3-3 Antibodies—The cDNA encoding *Dictyostelium* 14-3-3 was cloned via BamHI and SalI into pGEX-6P1 (GE Healthcare), expressed in bacteria (Rosetta, Novagen), and glutathione *S*-transferase-tagged 14-3-3 protein was purified via glutathione-Sepharose (Sigma). Polyclonal antibodies against *Dictyostelium* 14-3-3 were obtained by immunizing a female white New Zealand rabbit with purified glutathione *S*-transferase-tagged 14-3-3 following standard procedures.

Small Scale Pull-down of 14-3-3 Proteins Bound to TAP-tagged LrrB—For the small scale pull-down of TAP-tagged LrrB, 2 $\times$ 10^8 Ax2 cells transformed with either LrrB-CTAP or ΔCLrrB-CTAP were harvested and washed in KK2. For developmental stages, cells were initially disaggregated with a 23-guage needle. Cells were resuspended in 1 ml of TAP-Buffer A (10 mM Tris-Cl (pH 7.5 at 22 °C), 150 mM NaCl, 1% Nonidet P-40, 50 mM NaF, 0.5 mM phenylmethylsulfonyl fluoride, 1 mM sodium orthovanadate, 2 mM sodium pyrophosphate, 1 μg/ml pepstatin A, 1 mM benzamidine, 0.2 μM TLCK, and Complete protease inhibitor mixture (Roche Applied Science)) and incubated on ice for 3 min. The lysates were cleared by centrifugation, and the TAP-tagged protein complex was purified by incubating 1 ml of the supernatant with a 30-μl bed volume of IgG-agarose beads at 4 °C for 2 h. The beads were repeatedly washed with a total of 10 ml of TAP-Buffer B (10 mM Tris-Cl (pH 7.5), 150 mM NaCl, 0.1% Nonidet P-40, 1 mM sodium orthovanadate, 2 mM sodium pyrophosphate, 1 μg/ml pepstatin A, 1 mM benzamidine, 0.2 μM TLCK, 0.5 mM EDTA, 1 mM dithiothreitol, and Complete protease inhibitor mixture (Roche Applied Science)). The bound proteins were stripped from the

[3] Y. Yamada, personal communication.

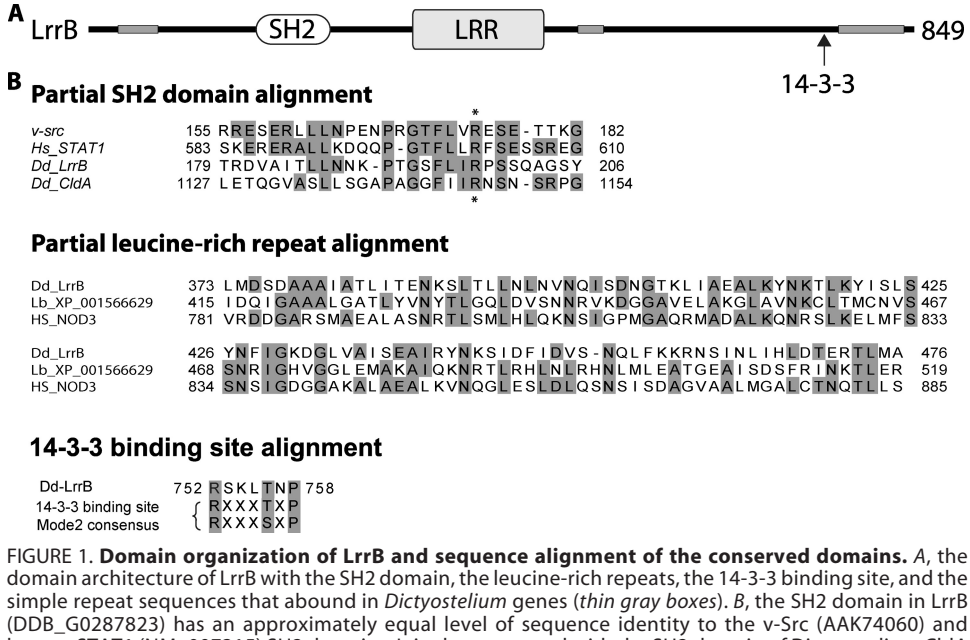

FIGURE 1. **Domain organization of LrrB and sequence alignment of the conserved domains.** *A*, the domain architecture of LrrB with the SH2 domain, the leucine-rich repeats, the 14-3-3 binding site, and the simple repeat sequences that abound in *Dictyostelium* genes (*thin gray boxes*). *B*, the SH2 domain in LrrB (DDB_G0287823) has an approximately equal level of sequence identity to the v-Src (AAK74060) and human STAT1 (NM_007315) SH2 domains. It is also compared with the SH2 domain of Dictyostelium CldA (DDB_G0278895). The SH2 invariant arginine is indicated by an *asterisk*. The leucine-rich repeat domain is aligned with similar domains from *Leishmania* ribonuclease inhibitor-like protein (XP_001566629) and human NOD3 (EAW85351). The 14-3-3 mode 2 consensus binding site was manually identified.

IgG-agarose by boiling the beads for 2 min with SDS-PAGE sample buffer. The amount of 14-3-3 pulled down was monitored by Western analysis of the eluted fractions, probing with 14-3-3 antibody, and by quantification with an Odyssey infrared imaging system (LI-COR Biosciences). The 14-3-3 pulldown was normalized by quantitating LrrB-CTAP in the corresponding crude lysate by Western analysis with just the IRDye^{TM} 800 goat anti-rabbit IgG (H&L) (Rockland Immunochemicals), which detects the protein A portion of the TAP tag, and then by quantitation of the LrrB-CTAP band.

Purification of TAP-tagged Protein Complexes—TAP purification was performed using 9×10^9 exponentially growing cells. These were harvested and starved for 4 h in KK2 at 1×10^7cells/ml. For pervanadate treatment, cells were harvested, resuspended at 2×10^7 cells/ml, and shaken with 1:200 pervanadate (prepared by mixing 5.65 μl of 30% (v/v) H_2O_2 with 500 μl of 200 mM sodium orthovanadate) for 10 min at 22 °C. Cells were harvested and lysed for 5 min on ice in 45 ml of TAP-Buffer A. Lysates were cleared by centrifugation (10,000 $\times$ *g* for 15 min at 4 °C), and the supernatant was mixed with a 300-μl bed volume of IgG-agarose beads (Sigma) by rotation at 4 °C for 2 h. The resin was applied into a 10-ml Poly-Prep chromatography column (Bio-Rad) and washed with 50 ml of TAP-Buffer B. The bound proteins were then cleaved from the drained resin using 200 units of tobacco etch virus protease (AcTEV, Invitrogen) in 2 ml of TAP-Buffer B with rotation overnight at 4 °C.

The tobacco etch virus protease-cleaved mixture was eluted from the IgG-agarose beads, and $CaCl_2$ was added to a final concentration of 2 mM and then diluted with 3 volumes of TAP-Buffer C (10 mM Tris-Cl (pH 7.5), 150 mM NaCl, 1% Nonidet P-40, 10 mM β-mercaptoethanol, 1 mM magnesium acetate, 1 mM imidazole, 2 mM $CaCl_2$, 1 mM sodium orthovanadate, 1 μg/ml pepstatin A, 1 mM benzamidine, 0.2 μM TLCK, and Complete protease inhibitor mixture (Roche Applied Science)) and batch-bound to a 500-μl bed volume of calmodulin affinity resin (Stratagene) in a 10-ml Poly-Prep chromatography column (Bio-Rad) rotating for 2 h at 4 °C. After washing the resin with 50 ml of TAP-Buffer C, any bound proteins were eluted with TAP-Buffer D (as TAP-Buffer C except that $CaCl_2$ is replaced by 2 mM EGTA) in multiple 440-μl fractions. A small sample of each fraction was used to monitor specific proteins eluted by Western analysis, and the remaining fraction was precipitated (4 volumes of acetone at −80 °C overnight) and the proteins were separated by SDS-PAGE on a precast 4–12% BisTris gel (Invitrogen) and visualized with a colloidal Coomassie staining kit (Invitrogen). Protein mass fingerprint data were obtained by matrix-assisted laser desorption ionization time-of-flight (tandem mass spectrometry) analysis.

Immunoprecipitation Assay—Ax2 cells, co-transformed with LrrB-GFP and CldA-CTAP or CTAP control, were harvested from vegetative cultures, washed in KK2, and then resuspended and lysed in Lysis Buffer (50 mM Tris-Cl (pH 8.0 at 22 °C), 150 mM NaCl, 1% (v/v) Triton X-100, 50 mM NaF, 2 mM EDTA, 2 mM sodium pyrophosphate, 1 mM sodium orthovanadate, 1 μg/ml pepstatin A, 1 mM benzamidine, and Complete protease inhibitor mixture (Roche Applied Science)) at 4×10^7 cells/ml on ice for 10 min. The lysates were centrifuged to remove insoluble material and then incubated with a 10-μl bed volume of Protein G-agarose Fast Flow (Upstate) at 4 °C for 30 min to preclear. Supernatants were incubated, with gentle rotation, with either mouse anti-GFP (Roche Applied Science) or rabbit anti-TAP for 1 h (3 μl in 1 ml) and then a 20-μl bed volume of Protein G-agarose Fast Flow for 2 h at 4 °C. The agarose resin was washed four times in 1 ml of Lysis Buffer. The resulting immune complexes were subjected to Western blotting and probed with either anti-GFP or anti-TAP antibodies as indicated.

RESULTS

LrrB Has a Novel Domain Organization

lrrB is predicted to encode a protein of 85,400 kDa. As with many *Dictyostelium* proteins (3), simple repeat sequences constitute a significant proportion of LrrB (Fig. 1*A*). LrrB contains an SH2 domain near the N terminus and leucine-rich repeats in its center (Fig. 1*A*). The leucine-rich repeats align best with members of the ribonuclease inhibitor-like family. The longest of the leucine-rich repeat protein alignments extend from the C terminus-proximal boundary of the SH2 domain to approxi-

mately residue 700 in LrrB. The expression of *lrrB* was analyzed by RT-PCR. It is expressed semiconstitutively, during growth and throughout development (Fig. 2).

An lrrB Disruptant (lrrB$^-$) Strain Grows Normally and Undertakes Early Development Correctly

An *lrrB* disruptant strain was created by homologous replacement using a gene disruption vector. Disruption was confirmed by PCR and Southern transfer analysis of genomic DNA (data not shown). *lrrB*$^-$ grows with a doubling time similar to that of the parental strain and develops in an outwardly normal manner up to the tipped aggregate stage. Subsequent development is delayed by several h, and misshapen fruiting bodies, often with the spore head incompletely raised up the stalk, are eventually formed (data not shown). We do not currently understand the reasons for these temporal and structural aberrations.

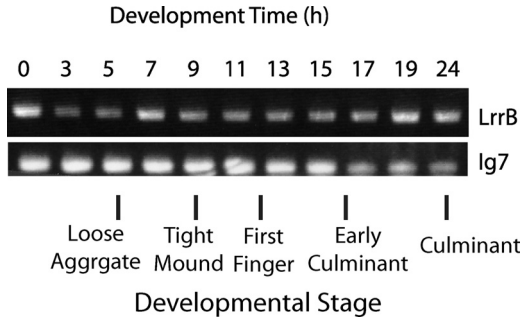

FIGURE 2. **Developmental time course of LrrB expression.** RNA samples were prepared from Ax2 cells, developing on filters on water agar and at the time points indicated. Semiquantitative RT-PCR was performed to assess the expression level with 260 ng of RNA for LrrB and 10 ng of RNA for Ig7, which was used as a loading control. Developmental stage marks indicate the approximate midpoint of development stage in Ax2. The *lrrB* primers were as follows: LrrB05 (5′-CTATGAAGAGAAAGTGCGAGTTATTTGG) (forward) and LrrB08 (5′-TCTCTTAAATCTTGCTCGATTGATG) (reverse); Ig7, 5′-TTACATTTATTAGACCCGAAACCAAGCG (forward) and Ig7rev (5′-TTCCCTTTAGACCTATGGACCTTAGCG) (reverse).

Gene Expression in the lrrB Disruptant Strain Is Aberrant during Growth

Although *lrrB* is expressed during growth, the *lrrB*$^-$ strain grows apparently normally. In order to determine whether there might be a subtle growth defect, parental and *lrrB*$^-$ cells, dividing in axenic medium, were subjected to genome-wide microarray analysis. Three separate biological experiments were performed, and each was analyzed using both directions of dye labeling. This yielded six data sets, and a list of all genes showing a 2-fold or greater change in all six sets is presented in Table 1. This is a rigorous inclusion criterion, and, reflecting this, only 12 genes were deemed to be underexpressed and only 13 genes overexpressed in the *lrrB*$^-$ cells.

The conclusions of the array data were confirmed for five selected genes using QPCR. Three of the genes were chosen for further investigation because they show a very large expression decrease in *lrrB*$^-$ cells: *cinB* (a predicted lipid esterase that was originally named H5 (19), *ttdA* (a predicted metallohydrolase), and *abcG10* (a predicted ABC transporter). Also, two genes of known function from the list of overexpressed genes were analyzed: *dscA* to *-C* (all three discoidin 1 mRNAs, detected using a primer pair predicted to hybridize to all three transcripts) and *prtB*, which is annotated as an orthologue of proteasomal subunit α 7-1. In all five cases, the QPCR data were in qualitative agreement with the microarray data, but the QPCR analysis often showed even larger parent to mutant differences than were observed in the array experiments (Fig. 3). By far the largest differences were in underexpression, with *cinB*, *abcG10*, and

TABLE 1

Summary of genome-wide microarray analysis comparing vegetative lrrB$^-$ and Ax2

Genes are presented that show a 2-fold or greater change in all three separate biological replicate experiments and an overall *p* value (adjusted to correct for the false discovery rate) less than 0.05. Full array data are available from ArrayExpress (available on the World Wide Web) under the accession code E-TABM-803.

ID at DictyBase	Gene name	Annotation	Change
			-fold
>2-Fold up			
DDB_G0291301		Flavin domain-containing protein	3.294
DDB_G0271666	*prtB*	Proteosomal α-subunit 7-1, cAMP-responsive gene p	3.138
DDB_G0273919	*dscA*	Discoidin IA	3.117
DDB_G0273915			2.99
DDB_G0273887	*dscB/C*	Discoidin	2.99
DDB_G0268212		Putative DEAD/DEAH box helicase-containing protein	2.603
DDB_G0285419	*cryS*	Crystal protein	2.585
DDB_G0273749		Similar to Dd histidine kinase DhkE	2.497
DDB_G0273557			2.462
DDB_G0273937			2.395
DDB_G0273921		Zinc-containing alcohol dehydrogenase (ADH)	2.362
DDB_G0273875	*cf50*	Component of counting factor complex	2.25
DDB_G0277201		Chitin binding domain	2.204
>2-Fold down			
DDB_G0291121	*cinB*	Vegetative specific H5, lipid esterase	0.053
DDB_G0290975		Highly similar to cinB	0.092
DDB_G0292986	*abcG10*	ABC type 2 transporter	0.178
DDB_G0288519			0.204
DDB_G0269630	*ttdA*	DNase/metallo-dependent hydrolase	0.228
DDB_G0291518			0.248
DDB_G0276383			0.262
DDB_G0290245	*psiC*	Similar to PreSpore-inducing factor *psiA*	0.274
DDB_G0269728	*ciao1*	Putative cytosolic iron-sulfur assembly protein	0.279
DDB_G0275161			0.374
DDB_G0282255		Carbohydrate-binding and zinc-binding domain-containing protein	0.403
DDB_G0293762		Carbohydrate-binding domain-containing protein	0.463

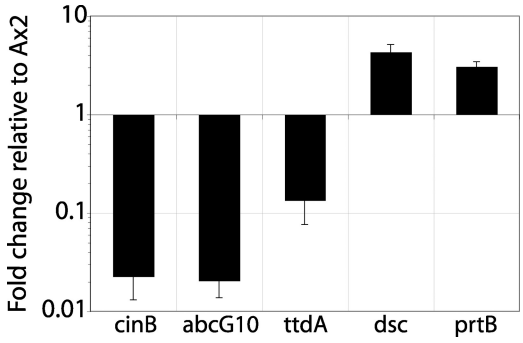

FIGURE 3. **Validation of selected microarray samples.** Vegetative RNA samples used for microarray analysis were analyzed for their level of expression of the five indicated genes using QPCR. The *bars* represent the expression level, expressed as the average -fold change in *lrrB*$^-$ cells relative to Ax2 cells. The *error bars* indicate S.E. from triplicate samples. Primers used were as follows: for ig7 (DDB_G0294034), TTACATTTATTAGACCCGAAACCAAGCG (forward) and AACAGCTATCACCAAGCTTGATTAGCC (reverse); for *cinB* (DDB_G0291121), CAAAGGAAGGTATGAAATGGTGTTGG (forward) and CCTTCAGAACTTAAGACATCGGTTTCAGC (reverse); for *dsc1A* to -C, GGTTTAGTTCAACTCCTCGCAAATGC (forward) and GAATTCACATCTTAATGAAATGTGACCATTCC (reverse); for *abcG10* (DDB_G0292986), CTCAACGTATTGCTTTAGGAAATGGTCA (forward) and CACTTGATTTCCTCCATGTTGATGGTC (reverse); for *ttdA* (DDB_G0269630), GTGCAAATTTAGCTGATAAATCATTTGAAAG (forward) and CTCCAACCGTTGAAAATAGTTCAACTAATC (reverse); for *prtB* (DDB_G0271666), TTAAATGCTGAAAAAGATGGAGAGTTTCTTG (forward) and GAAAACCAGTTTGAAAATCATTCCCAATATC (reverse).

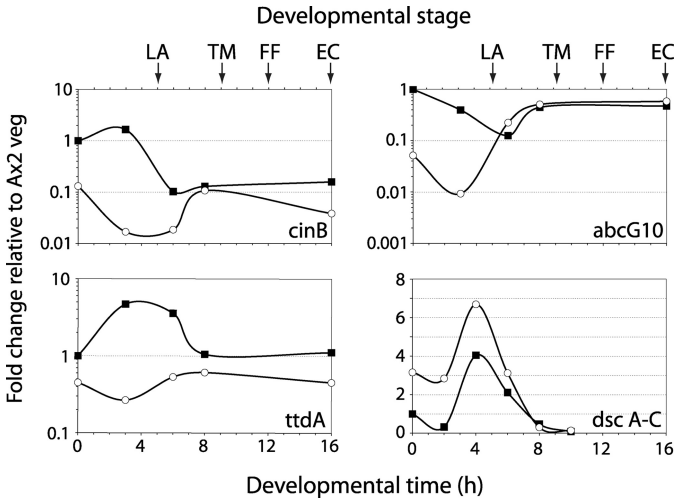

FIGURE 4. **Developmental time course of the expression pattern for selected genes.** Ax2 (■) and *lrrB*$^-$ (○) cells were developed on nitrocellulose filters on agar under uniform light conditions. RNA was prepared from samples harvested at the times indicated and analyzed for *cinB*, *abcG10*, *ttdA*, and *dscA* to *-C* expression levels using QPCR. Expression level is expressed as -fold change relative to vegetative Ax2. Developmental stage marks indicate the approximate midpoint of development stage in Ax2. *LA*, loose aggregate; *TM*, tight mound; *FF*, first finger; *EC*, early culminant.

ttdA displaying 44-, 49-, and 7-fold lower expression, respectively, in the *lrrB*$^-$ strain.

Developmental expression profiles were determined for *cinB*, *ttdA*, *abcG10*, and *dscA* to *-C* (Fig. 4). The former three genes are all underexpressed relative to the parental strain during early development, but later, mutant expression rises to approach or equal the parental level. In the case of *dscA* to *-C*, which is only expressed during early development, there is a uniformly higher level in the mutant strain.

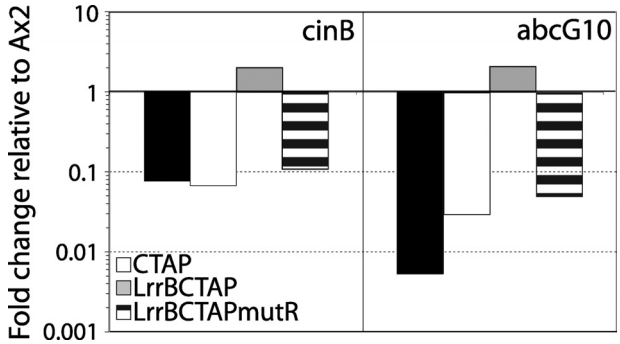

FIGURE 5. **Mutational analysis of the SH2 domain of LrrB.** *lrrB*$^-$ cells (*filled black bars*) were transformed with either the "empty" TAP-tagging vector (CTAP) (*empty bars*), a TAP-tagged *lrrB* gene (LrrB-CTAP) (*gray bars*), or a TAP-tagged mutant form (LrrB-CTAPmutR, in which arginine 198 of LrrB is substituted by alanine) (*cross-hatched bars*). RNA was prepared from vegetative transformed cells, and *cinB* and *abcG10* expression levels were measured using QPCR.

The SH2 Domain of LrrB Is Essential for Its Biological Function

An arginine residue, Arg^{175}, in v-Src makes critical contacts with Tyr(P) in the binding site (Fig. 1*B*). It is present in almost all SH2 domains, and when it is mutated, SH2 domain function is compromised. Hence, to assess the importance of the SH2 domain in LrrB, *lrrB*$^-$ cells were transformed with TAP-tagged (see below) expression constructs containing either the unmutated *lrrB* gene or a mutant form, LrrB-CTAPmutR, in which arginine 198 of LrrB is substituted by alanine. When LrrB-CTAP is expressed in *lrrB*$^-$ cells under control of the semiconstitutive actin 15 promoter, the expression level of the two most strongly *lrrB*-dependent genes, *cinB* and *abcG10*, increases (Fig. 5). In contrast, the Arg → Ala mutant form (LrrB-CTAPmutR) is inactive in rescuing expression of the two *lrrB*-dependent genes. Thus, the SH2 domain of LrrB is functionally essential for its early role in regulating gene expression.

LrrB Interacts in a Developmentally Regulated Manner with 14-3-3

In order to identify proteins that interact with LrrB, a TAP construct was generated. Expression of *lrrB* is directed by the actin 15 promoter, and a TAP tag was located at the C terminus of LrrB. The LrrB-CTAP construct was introduced into cells, using a Geneticin resistance cassette as a selectable marker, and TAP purification was performed using extracts from cells developed in suspension for 4 h. After the second, calmodulin affinity, purification step protein was eluted, concentrated, and analyzed by SDS-gel electrophoresis.

Western transfer using an anti-TAP antibody showed that the most abundant bands on the gel were LrrB-CTAP and its breakdown products (data not shown). Proteins identified, other than LrrB, (supplemental Fig. S1) were either highly abundant proteins, such as ribosomal proteins, actin, and β-tubulin, or proteins, such as heat shock protein 70, that might be expected to bind to denatured LrrB-CTAP. The one bound protein that seemed likely to be interacting in a meaningful way was the highly conserved regulatory protein 14-3-3 (20). An interaction of LrrB with 14-3-3 was confirmed using a small scale TAP tagging procedure, followed by Western transfer with a 14-3-3 antibody (Fig. 6*A*). The highest level of interaction

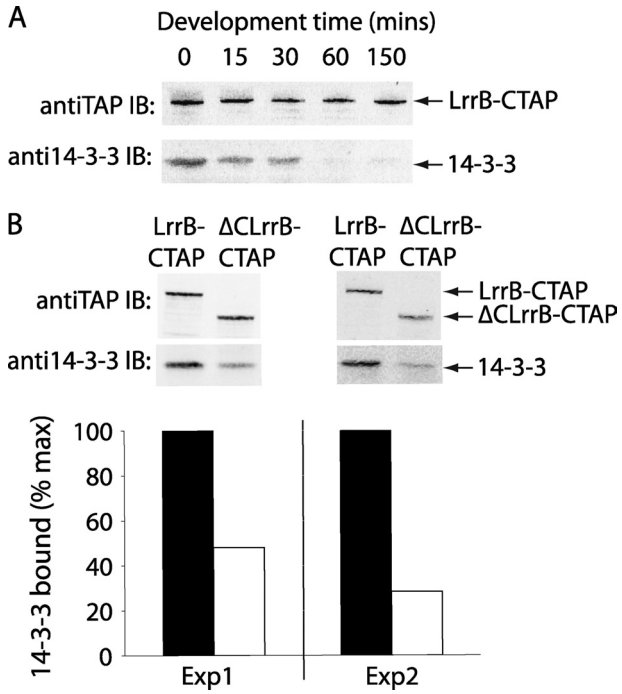

FIGURE 6. **Binding of 14-3-3 to LrrB-CTAP.** *A*, Ax2 cells transformed with LrrB-CTAP were harvested and shaken in suspension in KK2 at 1×10^7 cells/ml, and then aliquots were harvested at the time points indicated. LrrB-CTAP in the cell extracts was precipitated using IgG-agarose beads, and the 14-3-3 pulled down was detected by Western analysis using 14-3-3 antibody (*lower panel*). LrrB-CTAP in cell extracts was also assessed by Western analysis, using TAP antibody, to monitor LrrB-CTAP levels during the time course of the experiment. Similar results, with cells developed on agar, show the same drop in 14-3-3 binding, and low level was maintained up to 18 h. *B*, Ax2 cells transformed with either LrrB-CTAP or ΔCLrrB-CTAP were harvested during vegetative growth, and LrrB-CTAP or ΔCLrrB-CTAP in the cell extracts was precipitated (as above). Precipitated extracts were analyzed for 14-3-3 (by Western analysis) and quantified using an Odyssey infrared imaging system (LI-COR Biosciences). The amount of 14-3-3 pulled down was quantified then normalized to the LrrB-CTAP (or ΔCLrrB-CTAP) in corresponding cell extracts. Two independent experiments are shown. The *top two panels* show the LrrB-CTAP/ΔCLrrB-CTAP in cell extracts and 14-3-3 pulled down, and the *bar graph* represents the normalized values (*filled bars*, LrrB-CTAP; *empty bars*, ΔCLrrB-CTAP).

was during growth, and there was a rapid drop in binding during the first hour of development (Fig. 6*A*), to reach a basal level that was maintained through subsequent development (data not shown).

There are two recognized types of 14-3-3 binding site, mode 1 and 2, although many known binding sites do not fit well to either consensus (20). LrrB contains the sequence RSKLTNP, a perfect match to the mode 2 consensus, located near its C terminus (Fig. 1). When a C terminus-proximal region of 108 amino acids, containing the mode 2 binding site, was deleted, in construct ΔCLrrB-CTAP, there was a reduction in binding to 14-3-3 (Fig. 6*B*). 14-3-3 binds to proteins in a regulated fashion via their phosphorylated serine or threonine residues. Consistent with this, mutating the SH2 domain of LrrB did not decrease 14-3-3 binding, and treatment with pervanadate did not increase 14-3-3 binding (supplemental Fig. S3, *A* and *B*).

LrrB Interacts with Two Very Large Related Proteins

Aside from 14-3-3, the orthodox TAP tagging procedure yielded no obvious candidates for a functionally important interaction with LrrB. Therefore, we devised a more targeted approach, designed to identify proteins that interact with LrrB as part of an SH2 domain-phosphotyrosine signaling network. The approach was two-pronged.

Requirement for SH2 Domain Function—LrrB-CTAPmutR, the Arg → Ala mutant form of LrrB-CTAP, contains a mutation that inactivates its SH2 domain (Fig. 5). LrrB-CTAPmutR was used in TAP tagging purification in parallel with LrrB-CTAP to identify proteins that depend for their interaction with LrrB on the presence of a functional SH2 domain.

Requirement for Tyrosine Phosphorylation—Pervanadate is a tyrosine phosphatase inhibitor that causes high levels of phosphotyrosine protein modification in treated cells. In order to select for LrrB interactions that depend upon phosphotyrosine modification of the target proteins, we compared extracts from untreated and pervanadate-treated cells transformed with LrrB-CTAP.

A TAP purification using extracts from cells developed for 4 h in shaken suspension and expressing LrrB-CTAP or LrrB-CTAPmutR and either treated or not treated with pervanadate is shown in Fig. 7. A portion of the final eluate was analyzed by Western transfer using an anti-phosphotyrosine antibody. In the fractions derived from untreated cells, there are two proteins of high molecular weight (indicated as *b* and *c* in Fig. 7*B*). The extracts from cells exposed to pervanadate contain a much larger amount of what would appear to be, based upon their mobilities, the same two proteins and also a band of even higher molecular weight (marked *a* in Fig. 7*B*). Thus, inhibition of tyrosine phosphatase activity by pervanadate stimulates binding of these three proteins to LrrB-CTAP, suggesting that they interact with LrrB via SH2 domain-phosphotyrosine interactions. In confirmation of this notion, extracts from LrrB-CTAPmutR cells show little or no binding of the same high molecular weight species. Hence, the interaction of these tyrosine-phosphorylated protein species with LrrB is also dependent upon the presence of a functional LrrB SH2 domain.

The remainder of the fractions were concentrated, run on a preparative SDS gel, and stained with colloidal Coomassie (Fig. 7*C*). There are massive amounts of LrrB-CTAP protein (supplemental Fig. S2.) that preclude identification of the two lower molecular weight species visualized in Western analysis (the bands marked *b* and *c* in Fig. 7*B*). However, there is a band that is visible only in the pervanadate-treated sample that was selected on LrrB-CTAP. This has an apparent molecular mass of 130 kDa and so corresponds in approximate migration position to tyrosine-phosphorylated species "a" in the Western transfer analysis (Fig. 7*B*). *Band a* (Fig. 7*C*) was excised and subjected to tandem mass spectrometry, in parallel with the equivalent gel region taken from the control, non-pervanadate-treated sample. Peptides with highly significant scores derived from three proteins were uniquely detected in the pervanadate-treated LrrB-CTAP-purified sample.

One of the three proteins is ubiquitin, possibly linked to one of the other two identified proteins or perhaps linked to a protein for which no identification was made. One of the other identified proteins is CldA, one of the other two SH2 domain proteins for which a function has been neither assigned nor inferred (note that this is a revised terminology; it was previously called ChaA (3)). CldA contains an SH2 domain and, near

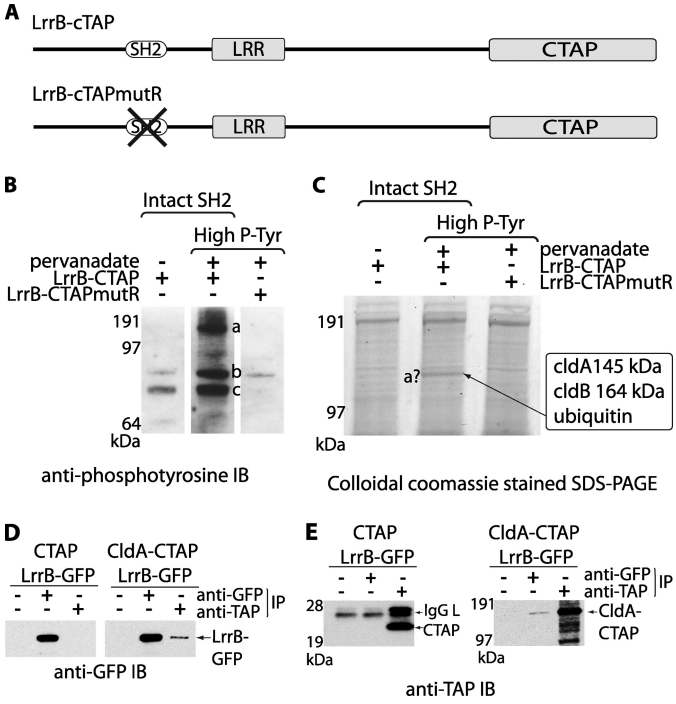

FIGURE 7. **Identification of proteins that bind to LrrB in an SH2 domain-dependent manner.** *A*, structure of LrrB-CTAP and LrrB-CTAPmutR. *B*, Western blot with an anti-phosphotyrosine antibody of samples from a TAP purification of LrrB-CTAP and LrrB-CTAPmutR after treatment with and without pervanadate. *Bands* marked *a*, *b*, and *c* are described in the text. *C*, portion of a colloidal Coomassie staining of a gel bearing a much larger amount of the same samples analyzed in *B*. The full colloidal Coomassie-stained gel is presented in supplemental Fig. S2. The 130 kDa band (marked as *a?*) was excised and subjected to tandem mass spectrometry, in parallel with the equivalent gel region taken from the control, non-pervanadate-treated sample. Three proteins were found to be unique to the pervanadate-treated LrrB-CTAP-purified sample. Neither large protein, DDB_G0278895 (CldA, 145 kDa) nor DDB_G0276091 (CldB, 164 kDa), migrate at the sizes expected. This could reflect anomalous migration because of their very large size, or it could indicate the presence of a secondary modification, such as ubiquitination; ubiquitin was the third protein present in *band a*. *D*, co-immunoprecipitation (*IP*) experiments carried out, using the antibodies stated, on extracts from Ax2 co-transformed with LrrB-GFP and CldA-CTAP (*right*) or with LrrB-GFP and CTAP as a control (*left*) and analyzed by Western blotting with an anti-GFP antibody. *E*, co-immunoprecipitation experiments carried out, using the antibodies stated, on extracts from Ax2 co-transformed with LrrB-GFP and CldA-CTAP (*right*) or with LrrB-GFP and CTAP as a control (*left*) and analyzed by Western blotting with an anti-TAP antibody. *IgG L*, IgG light chain carried over from the immunoprecipitation.

its C terminus, two tetracopeptide repeat sequences; these are also protein-protein interaction domains (Fig. 8*A*). The third protein identified as binding to LrrB-CTAP, CldB, does not contain an SH2 domain but does contain a region of homology to CldA (Fig. 8). This region is similar to a highly conserved sequence, recently designated the Clu domain because it is present in CluA-related mitochondrial clustering proteins (21, 22). Hence, the names we propose for the proteins are CldA and CldB (Clu domain A and Clu domain B).

Confirmation that LrrB and CldA interact was obtained by co-immunoprecipitation. Immunoprecipitation with anti-TAP antibody from extracts of cells overexpressing TAP-tagged CldA (CldA-CTAP) and GFP-tagged LrrB (LrrB-GFP) yielded LrrB-GFP (Fig. 7*D*). There was no equivalent band using extracts from cells overexpressing a CTAP control and LrrB-GFP. The complementary experiment was to perform immunoprecipitation with an anti-GFP antibody on extracts of cells overexpressing CldA-CTAP and LrrB-GFP. As expected, this yielded a CldA-CTAP band, whereas the CTAP control extract did not yield CTAP (Fig. 7*E*).

LrrB-regulated Genes Are Similarly Misregulated in a cldA Disruptant Strain (cldA)

A *cldA* disruptant strain was created by homologous gene disruption using a gene disruption vector. Disruption was confirmed by PCR of genomic DNA (data not shown). The mutant develops to completion, but a high proportion of the tight mounds go on to form doughnut-like structures as transitory intermediates (data not shown). The expression of the three genes that are down-regulated in the *lrrB* null strain, *cinB*, *ttdA*, and *abcG10*, was analyzed by QPCR using RNA from growing cells (Fig. 9). Expression in the *cldA*$^-$ strain was compared with the expression level in a random integrant from the same transformation and is presented alongside data for the *lrrB*$^-$ strain. Expression of the three genes is down-regulated in the *cldA*$^-$ strain, albeit less strongly than in the *lrrB*$^-$ strain.

DISCUSSION

The Domain Structure of LrrB Suggests That It Is an Adaptor Protein—The SH2 domain and the leucine-rich repeats are the only regions of LrrB that produce significant scores in a BLAST search, and between them they occupy almost all of the non-repetitive sequence. SH2 and leucine-rich repeat domains mediate protein-protein interactions and, in a search of genomic databases, LrrB is unique in possessing this particular domain combination. The leucine-rich repeats fall into the ribonuclease inhibitor-like family. This class of repeats, the LRR_RI family, is typically found in intracellular proteins rather than extracellularly on trans-membrane receptors (23). The *lrrB* gene is expressed at its highest level during growth, but there is continued expression throughout development. We believe, therefore, that LrrB is a novel form of soluble adaptor protein that functions during growth and throughout development. Repeated attempts to raise an antibody useful in immunolocalization of LrrB were unsuccessful.[4] Hence, we also attempted to determine the intracellular localization of a fusion construct, containing GFP linked to the C terminus of LrrB. Unfortunately, the fusion protein was extensively degraded within the cells. We do not therefore know the intracellular localization of LrrB and have used genetic and biochemical approaches to study it further.

LrrB Is a Regulator of Growing Cell and Early Developmental Gene Expression—Expression profiling of growing cells shows that the *lrrB*$^-$ strain is aberrant in its pattern of gene transcription. As might be predicted from the semiconstitutive expression profile of *lrrB* itself, gene expression in the *lrrB*$^-$ strain is also perturbed during development. For three of the genes that are underexpressed in the disruptant mutant, *cinB*, *abcG10*, and *ttdA*, there is a very large reduction indeed. This would suggest that the need for LrrB is specific and that LrrB plays a role in a defined pathway, rather than having some more generalized cellular function. Thus, combining these various pieces of information, we hypothesize that LrrB functions as an adap-

[4] C. Sugden and J. G. Williams, unpublished results.

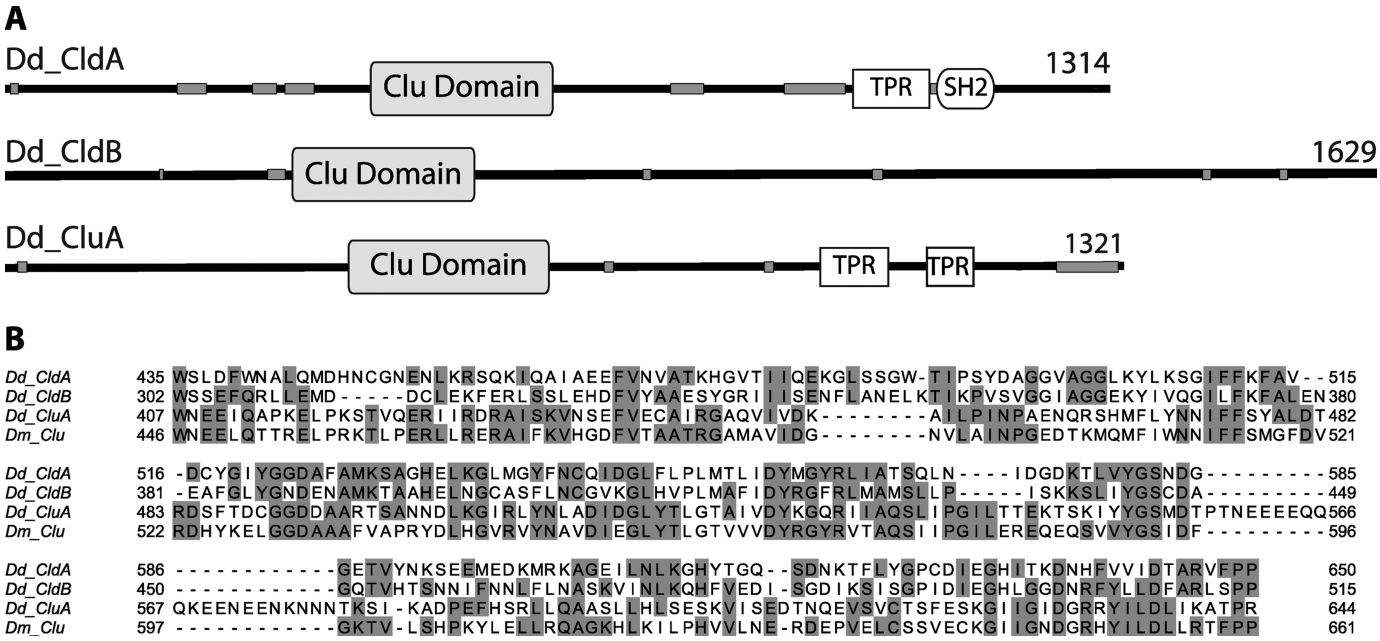

FIGURE 8. **The structures of CldA and CldB.** *A*, domain architecture of CldA and CldB. CldA and CldB share a common domain, the Clu domain. This domain was first identified in mitochondrial clustering proteins (21, 22), but it is also present in other proteins, such as ComB, a predicted Rab GTPase of unknown function (29). CldB shows no other hits in a BLAST search, but CldA contains an SH2 domain and several tetracopeptide repeats (*TPR*). CluA also contains tetracopeptide repeats in a similar relative position as CldA. Simple repeat sequences that abound in *Dictyostelium* proteins are represented by *thin gray boxes*. *B*, alignment of Clu domains from *Dictyostelium* CldA, CldB, and CluA with Clu domain from *Drosophilia* Clueless.

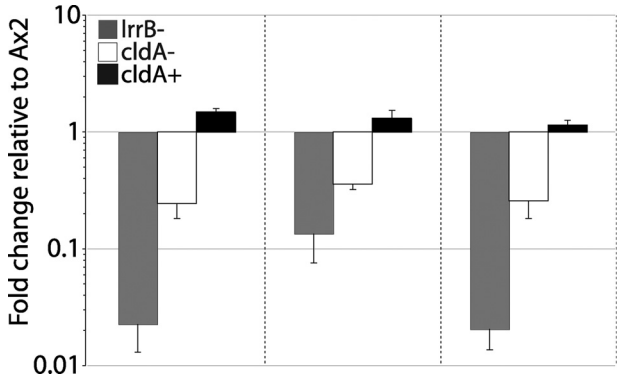

FIGURE 9. **Analysis of gene expression in a *cldA*$^-$ strain.** Vegetative RNA prepared from the *cldA*$^-$ strain (*empty bars*) and a random integrant (*cldA*$^+$; *black filled bars*) and Ax2, was analyzed for expression of the three genes that had been found to be down-regulated in the *lrrB*$^-$, using QPCR. The *bars* represent expression level, relative to Ax2, and the data for an *lrrB*$^-$ strain (Fig. 3) are presented alongside (*gray bars*) for comparison. *Error bars*, S.E. from triplicate experiments.

tor in a signaling pathway that controls specific gene expression events during growth and early development.

The *lrrB*$^-$ strain appears to develop normally up to the stage of tip formation. *lrrB*$^-$ also fails to culminate properly; the process is slow, and usually the fruiting body is incorrectly formed. Although array analysis of parental and *lrrB*$^-$ slug cell RNAs has not revealed any differences in individual gene expression of the magnitude found in growing cells, it seems likely that LrrB- also serves to control gene expression during multicellular development.

The *ttdA* and *abcG10* genes are uncharacterized, but *cinB* has previously been studied as a marker of the growth-development transition; it is transcriptionally repressed when cells enter development (24, 25). It was originally named H5 but was later renamed *cinB*. It encodes a lipid esterase domain-containing protein. CinB expression is known to be negatively regulated by GSK3 and also by ZAK1 (26), a tyrosine kinase that phosphorylates and activates GSK3 (27). Conversely, the *dsc1A* to *-C* genes are positively regulated by ZAK1 and GSK3 (26). Thus, the ZAK1-GSK3 signaling pathway functions oppositely to LrrB in regulation of both *cinB* and *dsc1A* to -C. This tentative link between pathways is given some credibility by the proportion of genes that are implicated; of just 23 genes or gene families regulated by LrrB, two (*cinB* and *dsc1A* to *-C*) are also regulated by ZAK1 and GSK3.

There Is Regulated Interaction of LrrB and 14-3-3—As a route to identifying other components of the LrrB signaling pathway, we used a proteomics approach. When TAP tagging was employed to identify proteins that interact with LrrB, the 14-3-3 protein was purified. Unusually among eukaryotic organisms, 14-3-3 is encoded by a single gene in *Dictyostelium* (28). There is a mode 2 14-3-3 binding site near the C terminus of LrrB, and deletion of a region containing this site substantially reduces 14-3-3 binding. Such incomplete inactivation is typical of 14-3-3-interacting proteins, which generally contain multiple, partially redundant 14-3-3 binding sites (20). In the N-terminal half of LrrB, there are two sequences (RVSSNDP and RMSFIP) that display some of the features of a 14-3-3 binding site and that could be responsible for the residual binding, but they have not been further investigated.

There is a rapid decrease in 14-3-3 binding during early development. This implies regulated dephosphorylation of one or more serine-threonine residues and strongly suggests some form of regulation of the activity of LrrB. However, the precise functional significance is unclear because a change in 14-3-3 binding can have disparate outcomes for the target protein,

including altered enzymatic activity, cellular localization, or stability (20).

Interaction of LrrB with CldA and CldB—Using an elaboration of the TAP tagging method, we identified two additional proteins that interact with LrrB, CldA, and CldB. Both proteins associate with LrrB in a manner that is dependent upon the SH2 domain of LrrB. Furthermore, the abundance of CldA and CldB in the complex dramatically increases when cells are pretreated with pervanadate. These facts suggest that formation of the complex is dependent upon an SH2 domain-phosphotyrosine interaction between LrrB and a phosphotyrosine in one of the two Cld proteins. There may well be additional SH2 domain-phosphotyrosine interactions because CldA itself contains an SH2 domain.

Aside from LrrB, there are only two functionally unassigned SH2 domain proteins in the *Dictyostelium* proteome. The fact that one of the two, CldA, forms part of a complex with LrrB is highly significant and is evocative of the interlinked SH2 domain signaling pathways of metazoa. If LrrB forms a complex with CldA and CldB, then one expectation might be that disruptant mutants in CldA or CldB would phenocopy *lrrB*$^-$ strains. In accord with this, a disruptant strain for CldA underexpresses the same three genes that are underexpressed during growth of the *lrrB*$^-$ strain. The fact that the extent of underexpression is less in the *cldA* null than in *lrrB* null strain could reflect the existence of another protein that is partially redundant with CldA.

What is the function of the complex? The domain structure of CldA may hold a clue. CldA contains a Clu domain, and there are tetracopeptide repeats near its C terminus. This is the same domain structure as the four, functionally defined, mitochondrial clustering proteins encoded by *Dictyostelium cluA*, *Saccharomyces clu1*, *Arabidopsis AtClu*, and *Drosophila clu* (21, 22, 30, 31). The *Drosphila clu* gene interacts genetically with and functionally phenocopies parkin, the orthologue of the human gene frequently responsible for familial Parkinson disease. The function of the Clu domain is unknown, but tetracopeptide repeats are believed to be protein-protein interaction domains. In the specific case of the Clu proteins, they have been suggested to compete with the tetracopeptide repeats on the kinesin light chain to prevent interaction of kinesin with its mitochondrial receptor (22). In *Drosophila*, the resultant clustering of mitochondria and possible increased oxidative damage lead to major changes in the expression of selected gene classes (22). There is no similar clustering of mitochondria in the *lrrB*$^-$,[4] but, perhaps, by analogy, the aberrations in gene expression during growth and early development of the *lrrB*$^-$ strain result from some global defect in cellular architecture that feeds back to regulate specific gene expression.

Acknowledgments—We thank Theresa Feltwell and Kay Jagels for technical assistance with the array analyses. Tandem mass spectrometry analysis was performed by the FingerPrints Proteomics facility at the School of Life Sciences, University of Dundee.

REFERENCES

1. Pawson, T., Gish, G. D., and Nash, P. (2001) *Trends Cell Biol.* **11,** 504–511
2. Liu, B. A., Jablonowski, K., Raina, M., Arcé, M., Pawson, T., and Nash, P. D. (2006) *Mol. Cell* **22,** 851–868
3. Eichinger, L., Pachebat, J. A., Glöckner, G., Rajandream, M. A., Sucgang, R., Berriman, M., Song, J., Olsen, R., Szafranski, K., Xu, Q., Tunggal, B., Kummerfeld, S., Madera, M., Konfortov, B. A., Rivero, F., Bankier, A. T., Lehmann, R., Hamlin, N., Davies, R., Gaudet, P., Fey, P., Pilcher, K., Chen, G., Saunders, D., Sodergren, E., Davis, P., Kerhornou, A., Nie, X., Hall, N., Anjard, C., Hemphill, L., Bason, N., Farbrother, P., Desany, B., Just, E., Morio, T., Rost, R., Churcher, C., Cooper, J., Haydock, S., van Driessche, N., Cronin, A., Goodhead, I., Muzny, D., Mourier, T., Pain, A., Lu, M., Harper, D., Lindsay, R., Hauser, H., James, K., Quiles, M., Madan Babu, M., Saito, T., Buchrieser, C., Wardroper, A., Felder, M., Thangavelu, M., Johnson, D., Knights, A., Loulseged, H., Mungall, K., Oliver, K., Price, C., Quail, M. A., Urushihara, H., Hernandez, J., Rabbinowitsch, E., Steffen, D., Sanders, M., Ma, J., Kohara, Y., Sharp, S., Simmonds, M., Spiegler, S., Tivey, A., Sugano, S., White, B., Walker, D., Woodward, J., Winckler, T., Tanaka, Y., Shaulsky, G., Schleicher, M., Weinstock, G., Rosenthal, A., Cox, E. C., Chisholm, R. L., Gibbs, R., Loomis, W. F., Platzer, M., Kay, R. R., Williams, J., Dear, P. H., Noegel, A. A., Barrell, B., and Kuspa, A. (2005) *Nature* **435,** 43–57
4. Williams, J. G., and Zvelebil, M. (2004) *Trends Plant Sci.* **9,** 161–163
5. Gao, Q., Hua, J., Kimura, R., Headd, J. J., Fu, X. Y., and Chin, Y. E. (2004) *Mol. Cell Proteomics* **3,** 704–714
6. Loomis, W. F., and Smith, D. W. (1990) *Proc. Natl. Acad. Sci. U.S.A.* **87,** 9093–9097
7. King, N., Hittinger, C. T., and Carroll, S. B. (2003) *Science* **301,** 361–363
8. Williams, J. G. (2003) in *Signal Transducers and Activators of Transcription (STATs): Activation and Biology* (Sehgal, P. B., Levy, D. E., and Hirano, T., eds) pp. 105–121, Kluwer Academic, Boston
9. Moniakis, J., Funamoto, S., Fukuzawa, M., Meisenhelder, J., Araki, T., Abe, T., Meili, R., Hunter, T., Williams, J., and Firtel, R. A. (2001) *Genes Dev.* **15,** 687–698
10. Langenick, J., Araki, T., Yamada, Y., and Williams, J. G. (2008) *J. Cell Sci.* **121,** 3524–3530
11. Zhukovskaya, N. V., Fukuzawa, M., Tsujioka, M., Jermyn, K. A., Kawata, T., Abe, T., Zvelebil, M., and Williams, J. G. (2004) *Development* **131,** 447–458
12. Araki, T., Langenick, J., Gamper, M., Firtel, R. A., and Williams, J. G. (2008) *Development* **135,** 1347–1353
13. Watts, D. J., and Ashworth, J. M. (1970) *Biochem. J.* **119,** 171–174
14. Pang, K. M., Lynes, M. A., and Knecht, D. A. (1999) *Plasmid* **41,** 187–197
15. Abe, T., Langenick, J., and Williams, J. G. (2003) *Nucleic Acids Res.* **31,** e107
16. Meima, M. E., Weening, K. E., and Schaap, P. (2007) *Protein Expr. Purif.* **53,** 283–288
17. Bloomfield, G., Tanaka, Y., Skelton, J., Ivens, A., and Kay, R. R. (2008) *Genome Biol.* **9,** R75
18. Olsen, R., and Loomis, W. F. (2005) *J. Mol. Evol.* **61,** 659–665
19. Singleton, C. K., Manning, S. S., and Ken, R. (1989) *Nucleic Acids Res.* **17,** 9679–9692
20. Mackintosh, C. (2004) *Biochem. J.* **381,** 329–342
21. Zhu, Q., Hulen, D., Liu, T., and Clarke, M. (1997) *Proc. Natl. Acad. Sci. U.S.A.* **94,** 7308–7313
22. Cox, R. T., and Spradling, A. C. (2009) *Dis. Model Mech.* **2,** 490–499
23. Kobe, B., and Kajava, A. V. (2001) *Curr. Opin. Struct. Biol.* **11,** 725–732
24. Singleton, C. K., Delude, R. L., and McPherson, C. E. (1987) *Dev. Biol.* **119,** 433–441
25. Singleton, C. K., Delude, R. L., Ken, R., Manning, S. S., and McPherson, C. E. (1991) *Dev. Genet.* **12,** 88–97
26. Strmecki, L., Bloomfield, G., Araki, T., Dalton, E., Skelton, J., Schilde, C., Harwood, A., Williams, J. G., Ivens, A., and Pears, C. J. (2007) *Eukaryot. Cell* **6,** 245–252
27. Kim, L., Liu, J., and Kimmel, A. R. (1999) *Cell* **99,** 399–408
28. Knetsch, M. L., van Heusden, G. P., Ennis, H. L., Shaw, D. R., Epskamp, S. J., and Snaar-Jagalska, B. E. (1997) *Biochim. Biophys. Acta* **1357,** 243–248
29. Kibler, K., Nguyen, T. L., Svetz, J., Van Driessche, N., Ibarra, M., Thompson, C., Shaw, C., and Shaulsky, G. (2003) *Dev. Biol.* **259,** 193–208
30. Fields, S. D., Conrad, M. N., and Clarke, M. (1998) *J. Cell Sci.* **111,** 1717–1727
31. Logan, D. C., Scorr, I., and Tobin, A. K. (2003) *Plant J.* **36,** 500–509